Technical Report on Local Indices of Physical Climate Uncertainty

Giuseppe Cavaliere Luca Fanelli Fabio Franceschini

May 2025

Abstract

We propose a methodology to construct local indices of physical climate uncertainty, focusing on monthly average temperature series across 44 grid points in Italy. Filtering out the trend of temperatures to apply the most suitable techniques, we use dynamic forecasting and factor modeling to construct time series of predictable forecast-error volatility and quantify conditional uncertainty. Our results show a significant rise in temperature uncertainty since the 1980s, especially in coastal areas.

Contents

Acknowledgements

This work was funded by the European Union - NextGenerationEU, in the framework of the "GRINS - Growing Resilient, INclusive and Sustainable project" (PNRR - M4C2 - I1.3 - PE00000018 – CUP J33C22002910001). The views and opinions expressed are solely those of the authors and do not necessarily reflect those of the European Union, nor can the European Union be held responsible for them.

1 Introduction

A critical aspect of climate change's impact on human activity is the uncertainty it generates. Uncertainty hampers the ability to plan and execute decisions, affecting resource allocation and overall welfare. This report presents a methodology to measure the uncertainty arising from increased monthly temperature dispersion, focusing specifically on the definition used by Jurado et al. (2015) in a macroeconomic context, i.e. the predictable component of the forecasting errors' volatility. The resulting indices provide high resolution in both temporal and geographical dimensions, making it possible to address two core questions: Have temperatures in Italy become harder to predict? Are these changes homogeneous across regions? These indices also support further applications, such as estimating the macroeconomic implications of climate uncertainty.

A central challenge in forming accurate conditional expectations of future temperatures for each location is the non-stationarity introduced by the well-known long-term phenomenon of global warming, and more broadly, climate change (Calvin et al., 2023). This challenge is at least twofold. First, non-stationarity requires specific econometric treatments to avoid shifts in the first moment biasing the estimates of dynamic models.[1] Second, large high-frequency fluctuations can obscure unit-root behavior in standard tests, potentially leading to the selection of inappropriate econometric models. To address these issues, the monthly temperature time series are first decomposed into trends and short-run components. The trends capture slow shifts in the first moment of the temperature distribution, while the short-run components reflect fluctuations whose dynamics are more closely related to the second and higher moments, and are also more likely to be stationary. Recognizing the ongoing debate on the nature of temperature trends (Chang et al., 2020), the decomposition is performed considering two classes of trends: (1) deterministic trends, obtained by estimating "hockey-stick" segmented time trends; and (2) stochastic trends, computed as 12-year moving-averages.

Predictions are obtained by estimating Dynamic Factor Models, which exploit the large number of time series to be predicted and the fact that both trend and short-run components exhibit a strong factor structure. For the short-run components, two methodologies are employed: a one-step procedure, as in Doz et al. (2012), and a two-step procedure, as in Doz et al. (2011). Both methodologies deliver high predictive accuracy, with the two-step procedure showing a notable advantage. For the stochastic trends, which are found to be integrated of order one, the methodology studied in Barigozzi et al. (2021) is applied. However, the uncertainty associated with the trend component is several orders of magnitude smaller than that of the short-run components – as expected.

The local temperature uncertainty indices are then obtained by squaring the temperatures' forecast errors and predict their logarithm, in line with stochas-

[1] It should be noted that shifts in the second moment of the temperature distribution (and higher ones), which are the focus of this work, can potentially make estimates inefficient, though they are still generally consistent. The inefficiency concern is also mitigated by the fact that the analysis relies on a long dataset with many observations.

tic volatility conventions. These series exhibit structural breaks in their mean, which are modeled explicitly. After de-meaning, as the residual factor structure appears weak, univariate time-series models are fit to the volatility series. Finally, an aggregate Italian temperature-uncertainty index is constructed by either averaging the regional series. The results reveal a pronounced rise in temperature-forecast uncertainty in Italy since the 1980s, with the most substantial increases observed along the coasts.

Obviously, forecast uncertainty depends on the underlying predictive model, and more sophisticated techniques may yield greater accuracy (Qasmi and Ribes, 2022). Nonetheless, given that one-month-ahead temperature forecasts are not readily and publicly available, a simpler time-series approach has the potential to more closely reflect the actual expectations of economic agents. It is also easier to replicate independently and serve as a benchmark for more sophisticated methods. A similar analysis was conducted by Mumtaz and Alessandri (2021), who, however, employed a different framework based on Bayesian methods, and used different data of yearly frequency, starting only in recent decades.

In Section 2, we present the data and the decomposition results; in Section 3 we illustrate the methodological framework; in Section 4 we show the key empirical facts emerging from the analysis; in Section 5 we conclude.

2 Data

2.1 Temperature data

The data consist of high-resolution land and ocean gridded temperature time series from Berkeley Earth. The analysis includes all grid points within a bounding box covering Italy, from 35.49°N to 47.5°N latitude and 6.63°E to 18.8°E longitude. These are "temperature anomalies", i.e. deviations from the local average between 1950 and 1980. The panel is balanced, comprising 44 time series (locations shown in Figure 1a), each with 1825 observations spanning from March 1872 to March 2024, as shown in Figure 1b.

Some descriptive statistics of the time series are reported in Table 1. It should be noted that no unit-root behavior is readily apparent, either from the plot or from the results of two standard tests. Specifically, while the Augmented Dickey-Fuller (ADF) test strongly rejects the presence of a unit root in all the series, the Kwiatkowski-Phillips-Schmidt-Shin (KPSS) test strongly rejects the null hypothesis of stationarity. Given the broader evidence for climate change, which directly implies some form of non-stationarity in environmental measurements, one might reasonably treat the series as integrated of order 1 from the outset. However, the ambiguity around their stationarity may carry over to the choice of predictive models, with standard cointegration tests, for example, suggesting the modeling of the temperature panel as a plain Vector Auto-Regression (VAR) *in levels*, as if the series were stationary. Since this work focuses on the uncertainty stemming from the dispersion of temperatures, the trends associated with the central tendency of the temperature distribution

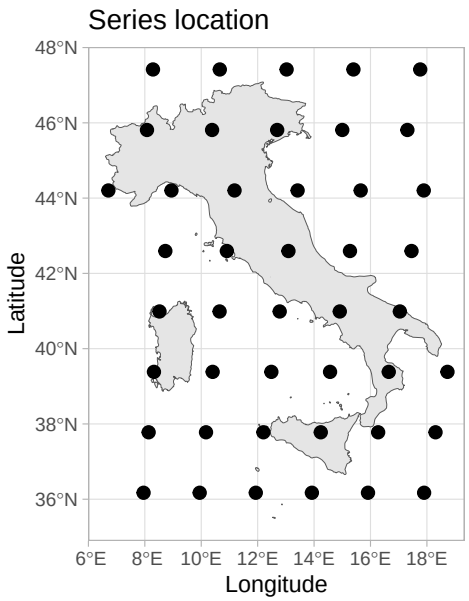

(a) Data geographical location

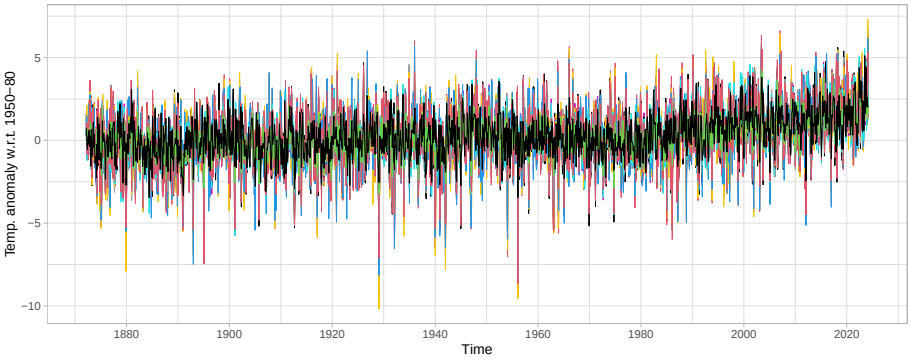

(b) Temperatures' time series

Figure 1: Overview of temperatures data.

Table 1: summary statistics of the temperature series. The ADF and the KPSS tests are performed without time trends.

Statistic	Mean	S.D.	ADF test	KPSS test
Min.	−4.53	2.54	−23.37***	3.43***
1st Qu.	−0.56	0.23	−20.96***	3.92***
Median	0.15	0.04	−17.25***	4.19***
Mean	0.17	0.03	−18.32***	4.12***
3rd Qu.	0.90	0.30	−15.67***	4.33***
Max.	4.30	1.34	−14.74***	4.60***

***: $p < 0.01$

are simply filtered out, to reduce ambiguity in the modeling strategy.

2.2 Temperatures' decomposition

As highlighted in Chang et al. (2020), there is an ongoing debate on the nature of temperature trends. Therefore, for robustness, both deterministic and stochastic trends are considered.

2.2.1 Deterministic trends

The anomalous increases in temperatures labeled as global warming are specific to recent decades. This implies that in a temperatures dataset of this length, any deterministic trend is expected to exhibit structural breaks, with an increase in the most recent period, forming what is often called a "hockey stick" (Mudelsee, 2019). Accordingly, the baseline deterministic trend is modeled as a segmented time trend, with the optimal break point selected via a grid search based on maximum likelihood, following Fong et al. (2017). The functional form is selected among flat-linear (flat before the break, and linear afterwards), flat-exponential, linear-linear, linear-exponential, and is chosen relying on the Bayes Information Criterion. For all the series the linear-exponential model results being the best one, with 38 changing points between 1970 to 1979, 4 between 1980 and 1989 and 2 between 2000 and 2009. The results are in Figure 2a.

2.2.2 Stochastic trends

The stochastic trends are identified using moving averages, which control the persistence of fluctuations (Ortu et al., 2013). The window length is set to 12 years, filtering out fluctuations less persistent than the solar cycle, whose period ranges from 10 to 12 years, and retaining only more persistent components in the trend. The trends are thus expected to primarily reflect dynamics in the first moment of the temperature distribution, while the variability in the de-trended series can be interpreted as the manifestation of dispersion in the distribution. It should be noted that stochastic trends defined in this way may still contain

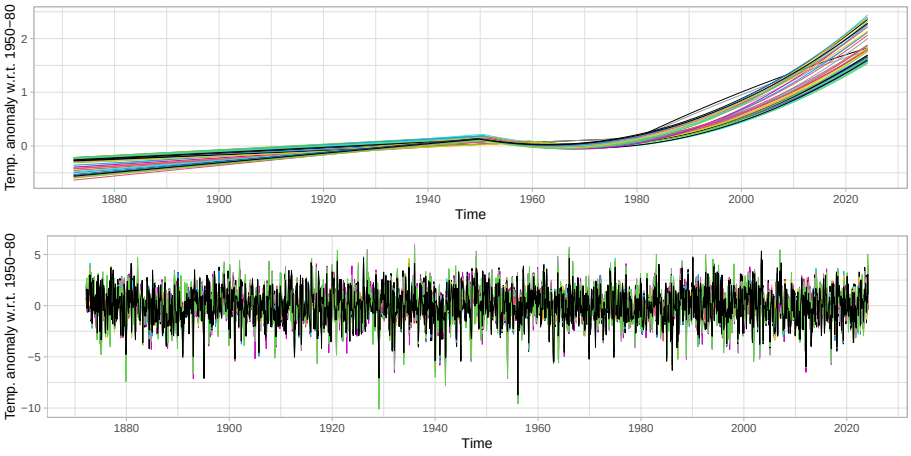

(a) Deterministic time-trend decomposition.

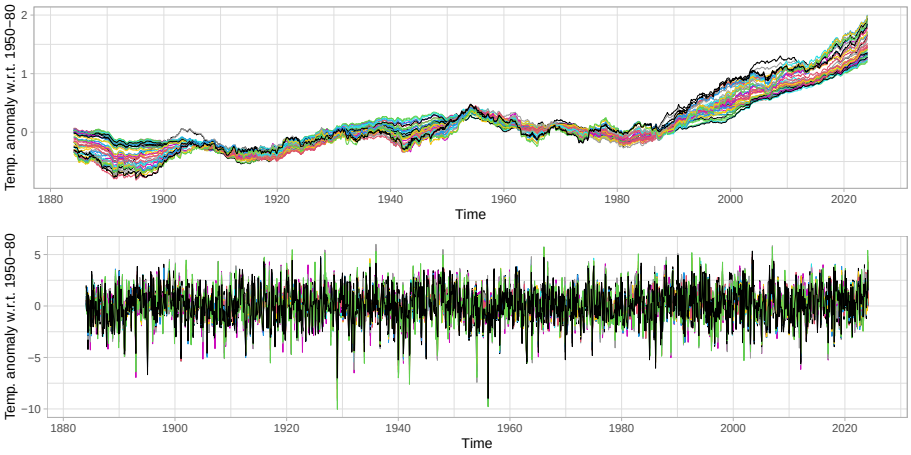

(b) Decomposition by 12-year moving average.

Figure 2: Trend and de-trended components for different filtering methods.

fluctuations that are periodic rather than permanent, such as those associated with lunar cycles, the Pacific Decadal Oscillation, the Atlantic Multidecadal Oscillation, and other known climate patterns, which exhibit periodicities ranging from about 20 years to millennial scales. Nonetheless, by applying this 12-year threshold, we filter out cycles with periodicities longer than 12 years, of which fewer than 13 full cycles would be observable in a 150-year dataset like ours. This ensures that the analysis focuses on fluctuations for which standard econometric techniques yield the most reliable results with the available data. Ultimately, the bulk of the uncertainty, the key focus of this study, is expected to arise from the de-trended series rather than the trends. This is rigorously verified by applying non-stationary techniques to the stochastic trends, showing that the uncertainty they contribute is orders of magnitude smaller than that arising from the short-term components. The results are in Figure 2b.

3 Econometric framework

The measurement of uncertainty follows a two-step procedure analogous to that employed in Jurado et al. (2015). First, dynamic predictions of temperature are generated using a Dynamic Factor Model (DFM). Second, the forecast errors are used to construct historical volatility time series, whose dynamic predictions constitute the measure of uncertainty. Differently from Jurado et al. (2015), in this work models volatility following a stochastic volatility approach,[2] and defines the uncertainty of a time series of interest y, at time t and horizon h, as

$$U_{y,t}(h) = \exp\left\{\frac{1}{2} \cdot \mathbb{E}\left[\ln\left(y_{t+h} - \mathbb{E}[y_{t+h}|I_t]\right)^2 \,|I_t\right]\right\}, \tag{1}$$

where I_t is the information set available at time t. Essentially, uncertainty is the component of the squared forecasting errors that can be predicted. The analysis is currently performed with h fixed at 1.

Obtained individual uncertainty time series, this can be aggregated in many different way, the most simple of which, the cross-sectional average per time period.

3.1 Temperatures Forecasting

The dataset consists of a balanced panel of stationary observations,

$$\boldsymbol{x}_t = \left(x_{1,t}, \ldots, x_{N,t}\right)', \quad t = 1, \ldots, T,$$

where $\boldsymbol{x}_t$ denotes the N-dimensional vector of de-trended temperature anomalies at time t, with $N = 44$ and no missing data.

To parsimoniously model the spatio-temporal dependence in the data, a reduced-rank Dynamic Factor Model (DFM) is employed. The observed process

[2] For a deeper discussion on this, see Taylor (1994).

$\boldsymbol{x}_t$ is assumed to be driven by a small number of latent common factors $\boldsymbol{f}_t \in \mathbb{R}^r$, with $r \ll N$, according to the following state-space system:

$$\boldsymbol{x}_t = \Lambda \boldsymbol{f}_t + \boldsymbol{\varepsilon}_t, \tag{2}$$

$$\boldsymbol{f}_t = \sum_{j=1}^{p} A_j \boldsymbol{f}_{t-j} + \boldsymbol{e}_t, \tag{3}$$

$$\mathbb{E}[\boldsymbol{\varepsilon}_t \boldsymbol{e}'_{t-k}] = 0 \qquad \forall k \ . \tag{4}$$

Here, $\Lambda \in \mathbb{R}^{N \times r}$ is the matrix of factor loadings; $\boldsymbol{\varepsilon}_t \in \mathbb{R}^N$ is the idiosyncratic component; and $\boldsymbol{e}_t \in \mathbb{R}^r$ is the vector of factor innovations. The dynamics of the common components are captured by a stationary VAR(p) process with autoregressive matrices $A_j \in \mathbb{R}^{r \times r}$, where the idiosyncratic and factor shocks are assumed to be mutually orthogonal at all leads and lags.

The number of latent factors is chosen following Alessi et al. (2010), while the estimation of the DFM and the recovery of the latent factors is implemented in two ways, which, delivering different prediction accuracy, ensures robustness of the final results. The first method is the two-step estimator of Doz et al. (2011), which leverages large-N asymptotics to produce consistent factor estimates. It begins with Principal Component Analysis to estimate static factors, which are then refined through a Kalman smoother applied to the dynamic system. The second approach is the one-step quasi-maximum likelihood estimator of Doz et al. (2012), which directly maximizes the Gaussian likelihood of the full state-space model via iterative Kalman filtering and smoothing. Given the balanced nature of the dataset and the focus on in-sample forecasting, the two-step procedure is adopted as the primary specification, while the one-step method serves as a robustness check.

3.2 Volatility Series Construction

Dynamic predictions of monthly temperatures, as specified in Section 3.1, are given by:

$$\mathbb{E}(\boldsymbol{x}_t | I_{t-1}) = \Lambda \sum_{j=1}^{p} A_j \boldsymbol{f}_{t-j}, \tag{5}$$

where $\boldsymbol{x}_t$ denotes the vector of observed temperatures, and $\boldsymbol{f}_{t-j}$ are the lagged factors driving the dynamics. The resulting one-step-ahead prediction errors at time t are defined as:

$$\boldsymbol{\omega}_t = \boldsymbol{x}_t - \Lambda \sum_{j=1}^{p} A_j \boldsymbol{f}_{t-j}. \tag{6}$$

Then, log-volatilities for each location i are constructed as:

$$v_{i,t} = \frac{1}{2} \log\left(\omega_{i,t}^2\right). \tag{7}$$

Stationarity of the log-volatility series $\{v_{i,t}\}$ is ambiguous for many locations, as will be illustrated later. This issue is addressed by applying a deterministic

de-trending procedure that allows for breaks in the mean. The rationale for this choice, along with supporting empirical evidence, is discussed in the following sections. Each log-volatility series is thus decomposed into a deterministic component and a zero-mean dynamic component:

$$v_{i,t} = \bar{v}_{i,t-1} + \tilde{v}_{i,t}, \tag{8}$$

where $\bar{v}_{i,t-1}$ denotes the known mean of the current regime, and $\tilde{v}_{i,t}$ is a stationary process around it.

As a result, the conditional expectations defining the uncertainty for location i at time t are given by:

$$\begin{aligned} U_{x_i,t}(1) &= \exp\left\{\mathbb{E}(v_{i,t+1}|I_t)\right\} &(9)\\ &= \exp\left\{\bar{v}_{i,t} + \mathbb{E}(\tilde{v}_{i,t+1}|I_t)\right\}, &(10)\end{aligned}$$

highlighting the need to model the dynamics of the stationary component of volatility.

3.3 Dynamic Volatility Predictions

Empirical analysis indicates that the de-trended log-volatility series $\{\tilde{v}_{i,t}\}$ exhibit only weak cross-sectional dependence (Alessi et al. (2010) would suggest employing 22 factors). Consequently, a multivariate approach would provide little additional explanatory power, and each series is modeled independently. The modeling framework relies on Seasonal Autoregressive Moving Average (SARMA) specifications, which capture both temporal dependencies and seasonal effects in the de-trended log-volatility series. For each series, the model is selected by minimizing the Akaike Information Criterion (AIC), ensuring an appropriate balance between fit and complexity. The general form of an SARMA$(p,q)(P,Q)_s$ model is:

$$\Phi_P(L^s)\phi_p(L)\tilde{v}_{i,t} = \Theta_Q(L^s)\theta_q(L)\varepsilon_{i,t}, \tag{11}$$

where:

- $\phi_p(L)$ and $\theta_q(L)$ denote the non-seasonal autoregressive and moving average polynomials of orders p and q,
- $\Phi_P(L^s)$ and $\Theta_Q(L^s)$ denote the seasonal AR and MA polynomials of orders P and Q with seasonal lag s,
- $\varepsilon_{i,t}$ is a white noise process.

The model selection procedure effectively determines the appropriate values of p, q, P, and Q for each series.

4 Empirical results

4.1 Temperatures' predictions

Factor structure De-trended temperatures exhibit a strong factor structure, with the first principal component accounting for over 70% of the total variance in both datasets – see the scree plots in Figure 3. In both cases, the optimal number of factors is four, collectively explaining over 90% of the variance.

Lag selection Relying on the Hannan–Quinn Information Criterion, the optimal p is 1 for all the models.

Model fit Figure 4 reports the R^2 for each time series and location. First, a substantial difference in the goodness of fit emerges between the two estimation methods – 1-step and 2-step – with the former ranging from as low as 52.5% to 99.9%, and the latter from 87.4% to 99.7%. Second, both methods exhibit a clear border effect, with fit improving toward more central locations. Third, the fit appears qualitatively higher over marine areas compared to terrestrial ones.

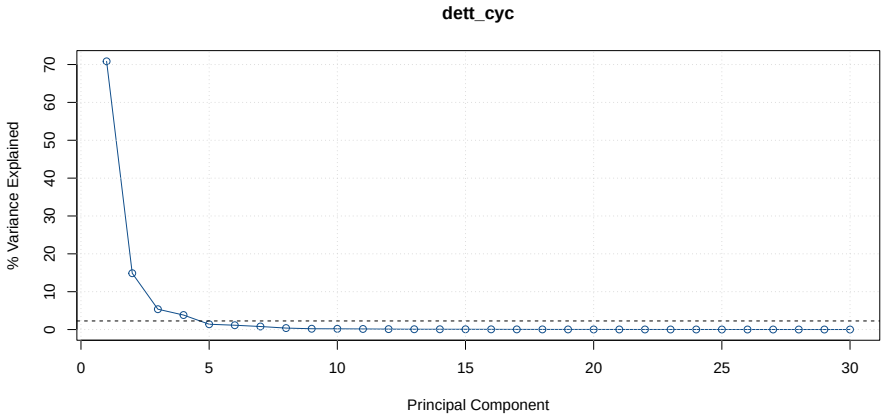

(a) Deterministic decomposition.

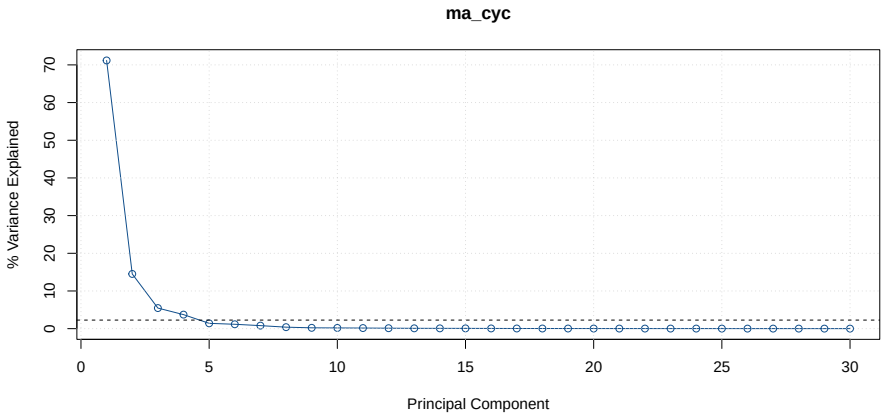

(b) Stochastic decomposition.

Figure 3: PCA screeplots. The dashed line marks the reciprocal of the number of units.

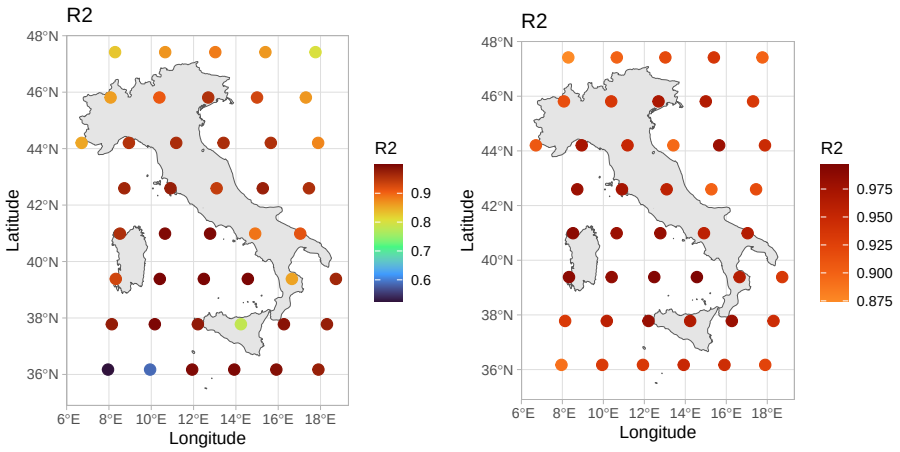

(a) Deterministic decomposition.

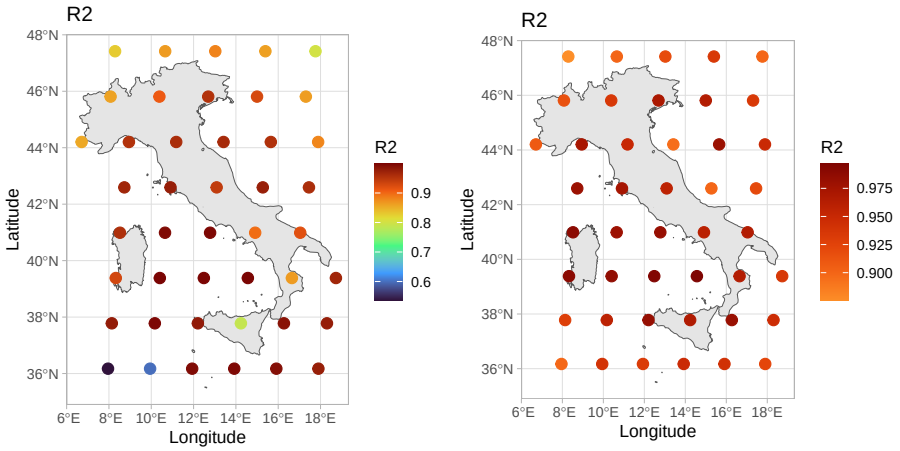

(b) Stochastic decomposition.

Figure 4: DFMs' R^2. On the left, 1-step estimation; on the right, 2-step estimation.

4.2 Intermediate Results on Volatility

Figure 5 illustrates the Italian volatility, obtained averaging each time period the volatility of all locations. Visually, there appears to be a remarkable increase in recent decades, which is confirmed by the formal test for a break in the mean of Andrews (1993). This highlights a potential non-stationarity of individual series too, which would impact the consistency of their predictions.

Non-stationarity of individual series is formally investigated starting with standard unit root tests first, whose results are shown in Table 2. Like results for the starting temperatures, these are once again ambiguous, with KPSS test suggesting a distinct possibility of many series actually being non-stationary. Next, structural breaks are controlled for by the means of the test studied in Bai and Perron (2003), looking both at breaks in the mean or time trends. AIC indicates models with breaks in the means to be always better than models with breaks in time trends. The test returns at least a break for most of the series, with some of them exhibiting up to 3 breaks. Anyway, for any de-trending and DFM-estimation method, most of the breaks happen between 1980 and 1989, as displayed in Table 3.

As explosive behavior result overall unlikely from visual inspection and unit-root tests, the non-stationarity is addressed by accounting for the changes in the mean of each series, while fitting S-ARMA models on de-trended series.

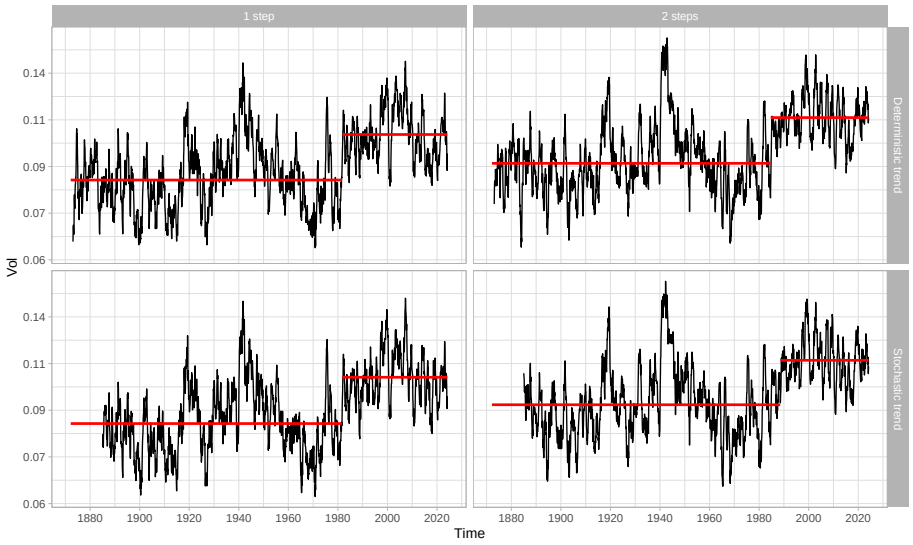

Figure 5: Italian average volatility.

Table 2: volatility stationarity – number of significant test statistics. The ADF and the KPSS tests are performed without time trends.

Trends	**Est. method**	**ADF test**	**KPSS test**
Deterministic	1-step	44	24
	2-step	44	24
Stochastic	1-step	44	25
	2-step	44	22

Table 3: count of breaks in mean by decade, as per Bai and Perron (2003). Decades start from year 0 and end in year 9.

Est. method	1900s	1910s	1920s	1930s	1940s	1950s	1960s	1970s	1980s	1990s
Deterministic trends										
1-step	2	5	0	2	1	3	0	4	9	3
2-step	1	2	3	4	2	7	1	1	14	3
Stochastic trends										
1-step	1	6	1	1	0	4	1	4	10	5
2-step	0	5	1	4	1	4	2	3	13	3

4.3 Uncertainty

Local Uncertainty Heterogeneity Figure 6 maps the average uncertainty across Italy, while Figure 7 displays the changes in uncertainty from 1970. Coastal regions, particularly along the Adriatic, together with the Aosta Valley and Friuli-Venezia Giulia, display the most significant rises in forecast error volatility. These local differences underscore the importance of disaggregated uncertainty measures for targeted policy interventions.

Italian Aggregate Uncertainty Figure 8 illustrates the Italian Uncertainty Index obtained as a cross-sectional average at each time period. It inherits a remarkable increase in after 1980 from many individual series, which also happen to be contemporaneous to the sharp rise in average temperatures of the last decades.

For robustness, in Figure 8 it is also displayed a similar index, obtained from fitting a I(1) DFM in the style of Barigozzi et al. (2021). As expected, the uncertainty from the stochastic trends contributes significantly less and, as such, can be effectively ignored in studying uncertainty dynamics.

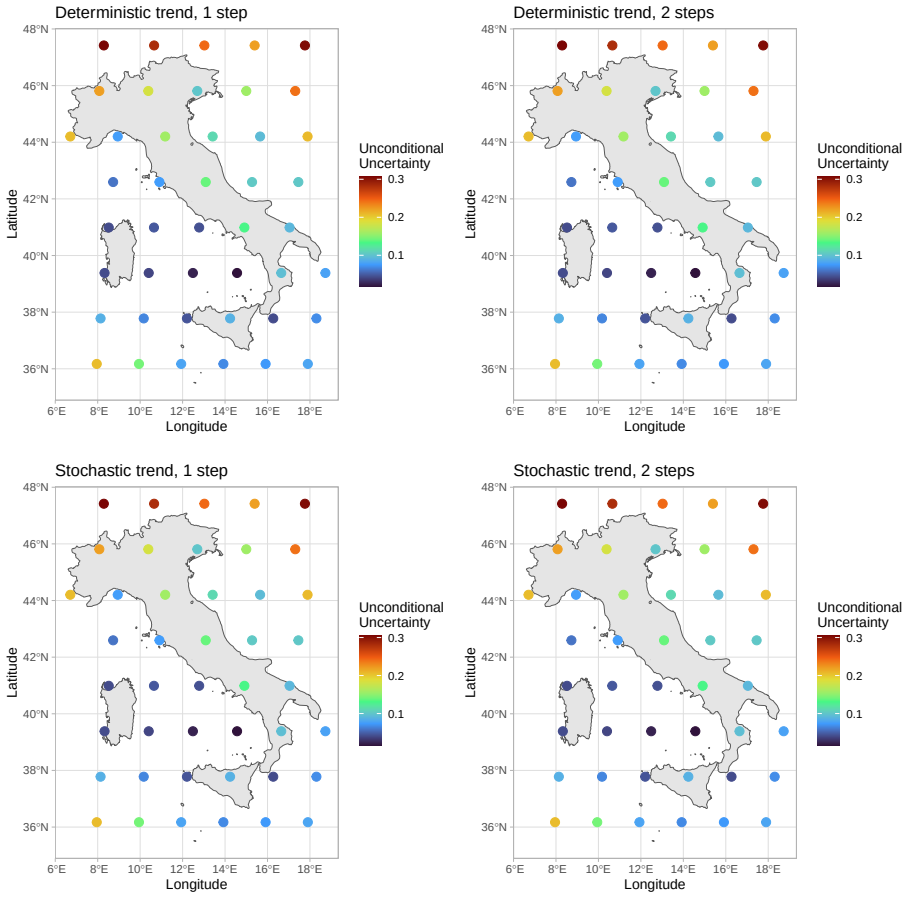

Figure 6: local average uncertainties.

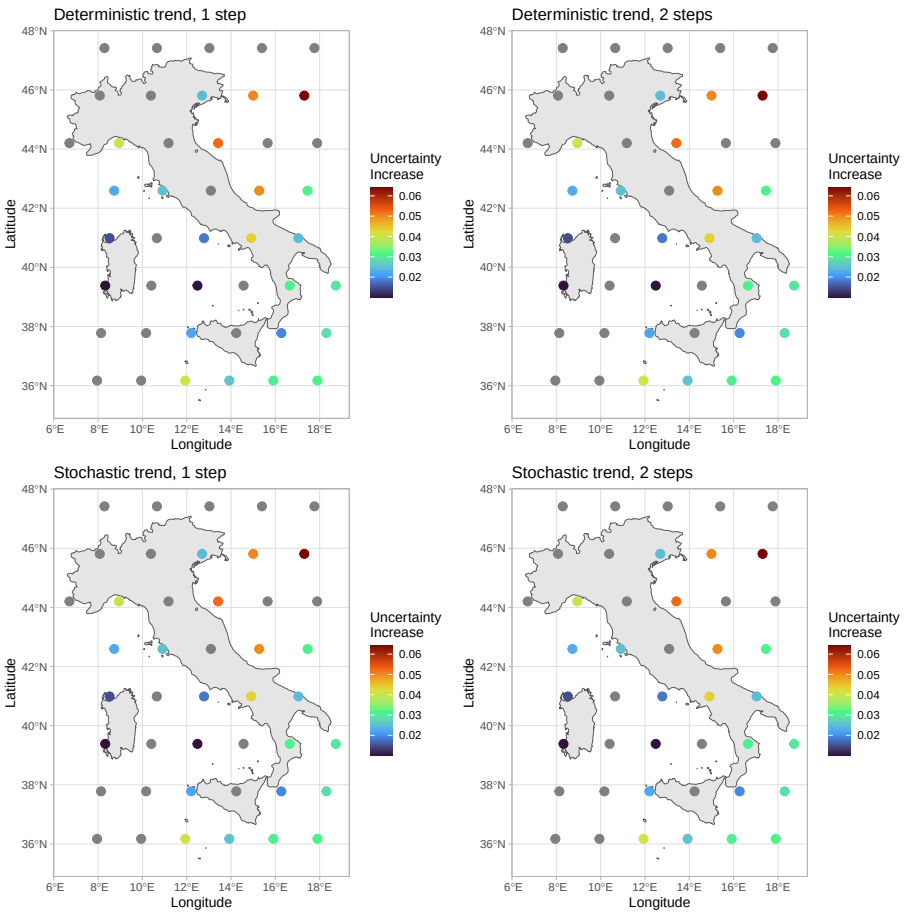

Figure 7: changes in uncertainty since 1970. Gray dots are for locations where no significant change occurred.

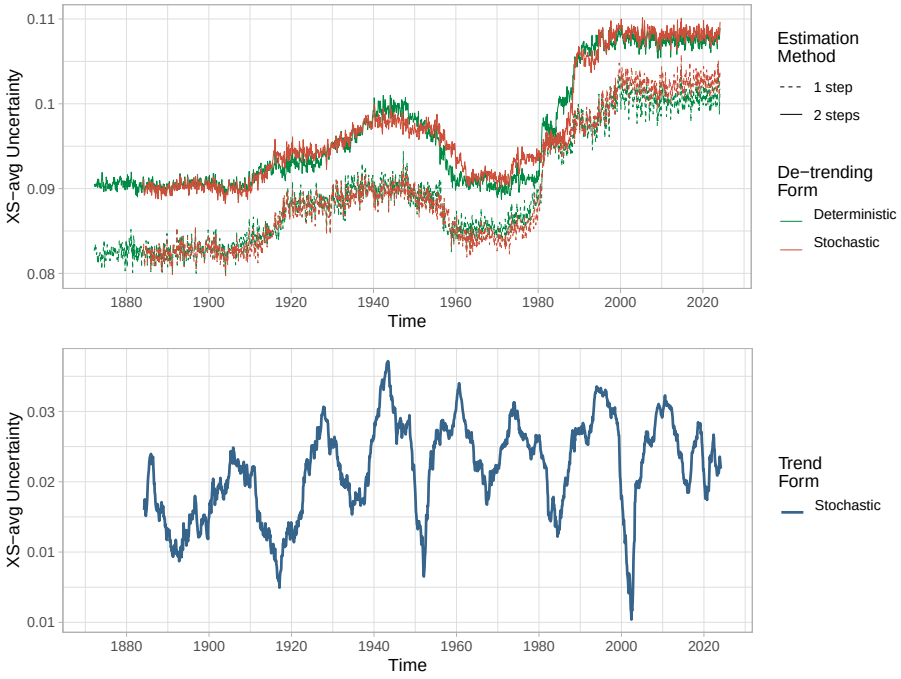

Figure 8: Aggregate Italian Uncertainty. Above, the uncertainty from the short-term components of temperatures; below, the uncertainty from the stochastic trends.

5 Conclusion and Perspectives

This study presents a methodological framework for measuring local physical climate uncertainty through a dynamic forecasting approach and subsequent volatility estimation. The significant rise in uncertainty – especially in key coastal regions of Italy – highlights both the challenges and the critical need for informed policy responses.

Future research should extend this framework to other climatic variables and geographical regions, as well as elucidate the economic impacts of climate uncertainty, which theoretical studies such as Cai (2021) have already highlighted as an important channel in the climate-economy relationship. On this specific point, particular care will be needed to control for reverse causality, given the apparently positive relationship suggested by the reduced-form estimations, as shown in Figure 9.

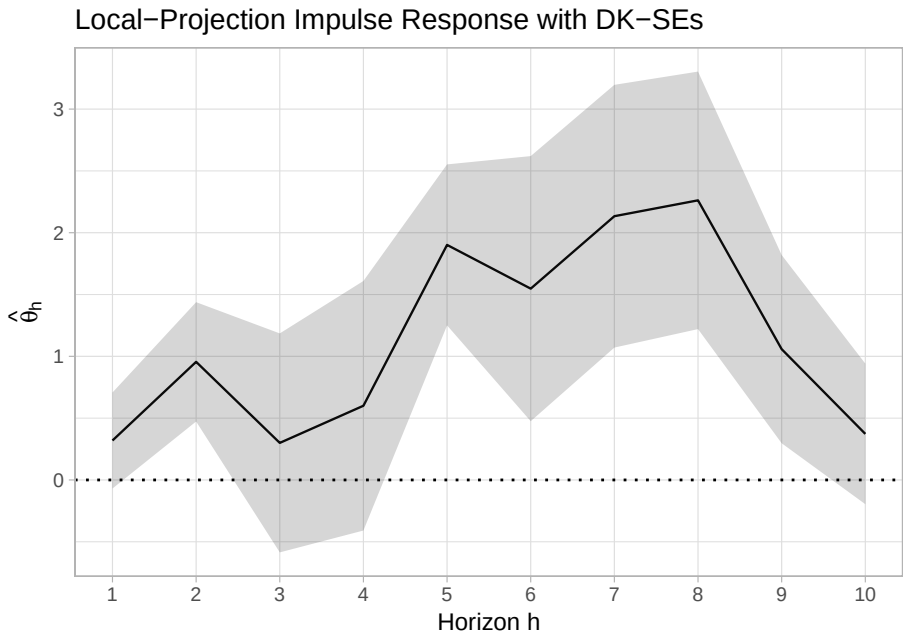

Figure 9: dynamic relation with regional GDP. Estimates obtained as in Bilal and Känzig (2024), adding global temperature-level shocks among controls.

A Supplementary materials

Supplementary material associated with this article can be found, in the online version, at *doi/grins link*

References

Alessi, L., Barigozzi, M., Capasso, M., 2010. Improved penalization for determining the number of factors in approximate factor models. Statistics & Probability Letters 80, 1806–1813. doi:10.1016/j.spl.2010.08.005.

Andrews, D.W.K., 1993. Tests for parameter instability and structural change with unknown change point. Econometrica 61, 821–856. doi:10.2307/2951764.

Bai, J., Perron, P., 2003. Computation and analysis of multiple structural change models. Journal of Applied Econometrics 18, 1–22. doi:10.1002/jae.659.

Barigozzi, M., Lippi, M., Luciani, M., 2021. Large-dimensional dynamic factor models: Estimation of impulse-response functions with i(1) cointegrated factors. Journal of Econometrics 221, 455–482. doi:10.1016/j.jeconom.2020.05.004.

Bilal, A., Känzig, D.R., 2024. The Macroeconomic Impact of Climate Change: Global vs. Local Temperature. Technical Report 32450. National Bureau of Economic Research. doi:10.3386/w32450.

Cai, Y., 2021. The role of uncertainty in controlling climate change, in: Oxford Research Encyclopedia of Environmental Economics. Oxford University Press. doi:10.1093/acrefore/9780190625979.013.573.

Calvin, K., et al., 2023. IPCC, 2023: Climate Change 2023: Synthesis Report. Contribution of Working Groups I, II and III to the Sixth Assessment Report of the Intergovernmental Panel on Climate Change. Synthesis Report. Intergovernmental Panel on Climate Change (IPCC). doi:10.59327/IPCC/AR6-9789291691647. edition: First.

Chang, Y., Kaufmann, R.K., Kim, C.S., Miller, J.I., Park, J.Y., Park, S., 2020. Evaluating trends in time series of distributions: A spatial fingerprint of human effects on climate. Journal of Econometrics 214, 274–294. doi:10.1016/j.jeconom.2019.05.014.

Doz, C., Giannone, D., Reichlin, L., 2011. A two-step estimator for large approximate dynamic factor models based on kalman filtering. Journal of Econometrics 164, 188–205. doi:10.1016/j.jeconom.2011.02.012.

Doz, C., Giannone, D., Reichlin, L., 2012. A quasi–maximum likelihood approach for large, approximate dynamic factor models. Review of Economics and Statistics 94, 1014–1024. doi:10.1162/REST_a_00225.

Fong, Y., Huang, Y., Gilbert, P.B., Permar, S.R., 2017. chngpt: Threshold regression model estimation and inference. BMC Bioinformatics 18, 454. doi:10.1186/s12859-017-1863-x.

Jurado, K., Ludvigson, S.C., Ng, S., 2015. Measuring uncertainty. American Economic Review 105, 1177–1216. doi:10.1257/aer.20131193.

Mudelsee, M., 2019. Trend analysis of climate time series: A review of methods. Earth-Science Reviews 190, 310–322. doi:10.1016/j.earscirev.2018.12.005.

Mumtaz, H., Alessandri, P., 2021. The macroeconomic cost of climate volatility. SSRN Electronic Journal doi:10.2139/ssrn.3895032.

Ortu, F., Tamoni, A., Tebaldi, C., 2013. Long-run risk and the persistence of consumption shocks. Review of Financial Studies 26, 2876–2915. doi:10.1093/rfs/hht038.

Qasmi, S., Ribes, A., 2022. Reducing uncertainty in local temperature projections. Science Advances 8, eabo6872. doi:10.1126/sciadv.abo6872.

Taylor, S.J., 1994. Modeling stochastic volatility: A review and comparative study. Mathematical Finance 4, 183–204. doi:10.1111/j.1467-9965.1994.tb00057.x.